CRYSTAL GROWTH & DESIGN

Article

pubs.acs.org/crystal

Controlling the Assembly of C2-Symmetric Molecular Tectons Using a Thiocarbamate Appended Carbocyclic Cleft Molecule Analogous to Tröger's Base

Natasha H. Slater,[†] Benjamin R. Buckley,[†] Mark R. J. Elsegood,*[,†] Simon J. Teat,[‡] and Marc C. Kimber*[,†]

[†]Department of Chemistry, Loughborough University, Loughborough, LE11 3TU, United Kingdom

[‡]ALS, Berkeley Laboratory, 1 Cyclotron Road, MS2-400, Berkeley, California 94720, United States

Supporting Information

ABSTRACT: By way of appending the C_2-symmetric carbocyclic cleft diol with thiocarbamates with varying substituents, significant control of the hydrogen bonded network can be achieved. Smaller alkyl substituents lead to the formation of stacked columns of components with the apex of one molecule suitably aligned in the cleft of a second. Aryl substituents, however, lead to the formation of ribbons via an H-bonding network. Additionally, the packing of these ribbons into networks is considerably different between the enantiopure and racemic clefts, with the latter giving rise to channels within the crystal structure.

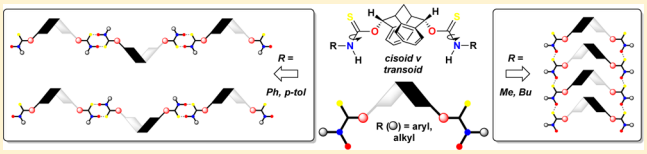

INTRODUCTION

The carbocyclic diol cleft molecule **1**[1−3] has become a surrogate for Tröger's base (**2**) in catalysis,[4] supramolecular chemistry,[5−7] and chiral recognition (Figure 1).[8−11] It is analogous to Tröger's base as it contains a C_2-symmetric axis, a chiral cavity with a defined geometry and a rigid, predictable structure. This gives **1** a predictable V-shape, whose angle (θ) can vary between 83.4° and 104.3° depending on the substitution on the aromatic ring.[12,13] The advantages of **1** over Tröger's base lie in the diol, with the two hydroxyl groups being pointed into the interior of the cleft giving the ability, via hydrogen bonding, to orientate and organize substrates into this uniquely chiral cavity. We have previously emphasized the practicality of **1** by appending the hydroxyl groups with pyridyl functionality, as well as highlighting the self-assembly of these pyridyl adducts with phenylboronic acid to yield bis-boroxine substrates, with the 4-pyridyl analogue being fully characterized by single crystal X-ray analysis emphasizing the chiral space.[14,15]

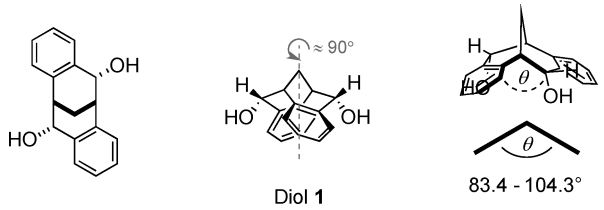

Figure 1. C_2-centrosymmetric chiral cleft diol **1**.

The capacity to be able to confidently predict crystal packing to facilitate the design of new solids with sought-after physical properties has been central to the evolution of crystal engineering.[16−18] Furthermore, the ability to control secondary and tertiary structure within crystal packing has enormous potential in the development of new functional materials and devices. Molecular tectonics[19−22] is the analysis of molecular crystals and their subsequent formation of networks, and as a consequence the tecton is defined as a construction unit with defined structural and energetic attributes that can control assembly via programmed molecular recognition processes. Consequently, the identification of new three-dimensional chiral molecules, or tectons, with rigid, predictable structures opens further prospects in expanding the scope of crystal engineering.

Akin to Tröger's base (**2**),[23,24] diol **1** can pack, in the solid state, in four possible forms **M1**, **M2**, **M3**, and **M4**, all of which are primarily driven by weak van der Waals and $\pi-\pi$ interactions (Figure 2).[25]

Conversely, thiocarbamates (**3**), like amides, form networks based on stronger hydrogen bonding, which is, in part, controlled by their configuration, with the *cisoid* form **3a** leading to synthon **4**, and the *transoid* form **3b** leading to synthon **5** (Scheme 1).[26,27]

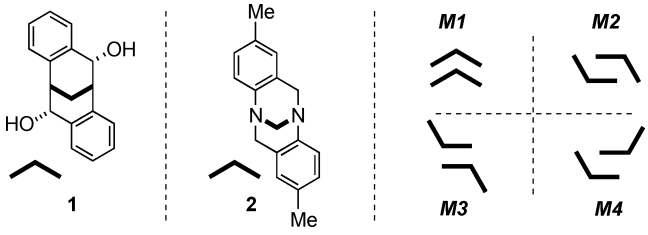

Figure 2. Control of crystal packing in chiral cleft diol **1**.

Received: March 9, 2016
Revised: April 21, 2016

DOI: 10.1021/acs.cgd.6b00388
Cryst. Growth Des. XXXX, XXX, XXX−XXX

Scheme 1. Control of Crystal Packing in Thiocarbamate 3

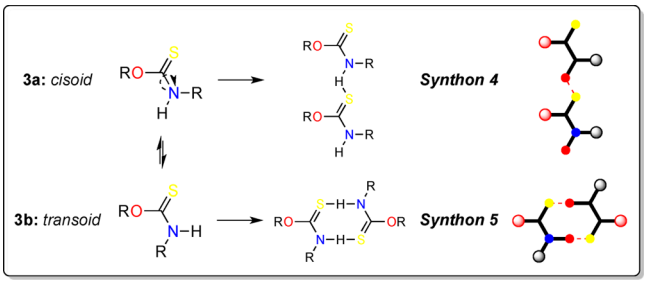

In an effort to regulate the crystal packing of chiral cleft **1**, we envisaged appending the diol with a variety of thiocarbamates (alkyl and aryl, Scheme 2, **6**). The crystal packing of these

Scheme 2. Targeted Thiocarbamates

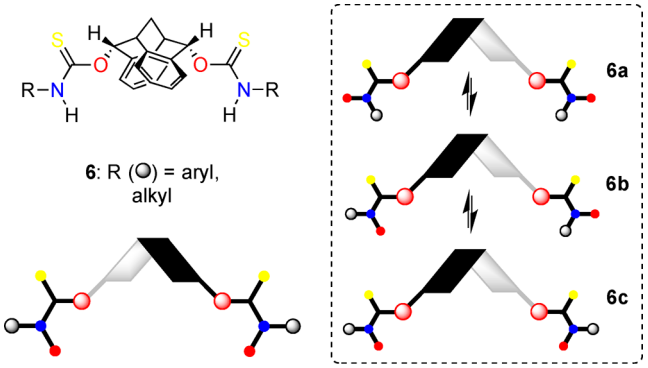

derivatives would then be primarily defined by the orientation of the thiocarbamate (*cisoid* and/or *transoid*) that is accurately described by **6a** ↔ **6b** ↔ **6c**. This would serve two purposes: (a) to allow the confident prediction of the crystal packing of **6**, therefore demonstrating this scaffold as a potential tecton; (b) to demonstrate that novel crystalline solids with predictable chiral environments can be formed from analogues of **1**.

RESULTS AND DISCUSSION

Preparation of Thiocarbamate Appended Clefts. The synthesis of the thiocarbamate cleft derivatives began with obtaining multigram quantities of the parent cleft diol **1**, and this was achieved as reported previously (Scheme 3).[2] This racemic diol could then be converted to the *bis*-thiocarbamate by treatment with NaH and excess isothiocyanate. This was accomplished with phenyl, tolyl, 3,5-ditrifluoromethylphenyl, methyl, and butyl isothiocyanates giving the desired compounds (±)-**10a-e** in moderate to good yields. In addition to the racemic thiocarbamates, enantiopure tolyl thiocarbamate was also prepared (Scheme 3). This was achieved by synthesizing the enantiopure diacid (+)-**8** via resolution of its racemate with quinine. This enantiopure diacid was then converted to the thiocarbamate, delivering enantiopure (+)-**10b**.

X-ray Crystallographic Analysis. Single crystal X-ray analysis was performed on phenyl (±)-**10a**, tolyl (±)-**10b**, 3,5-ditrifluoromethylphenyl (±)-**10c**, methyl (±)-**10d**, and butyl (±)-**10e** thiocarbamates. Additionally, single crystal X-analysis was also performed on the enantiopure tolyl (+)-**10b** analogue as a comparison with its racemic analogue. Crystal data, H-bond geometry, and 50% ORTEP plots are presented in the Supporting Information, and crystallographic procedures are described in the Experimental Section.

The crystal structure of the racemic phenyl-amino-thiocarbamate cleft (±)-**10a** illustrates the rigid cleft framework and the position of the two appending phenyl-amino-thiocarbamate units that are orientated toward the interior of the cleft (Figure S1). Interestingly, the sulfur and thiocarbamate N–H groups are pointing outward away from the cleft cavity such that only the aromatic phenyl groups are directed inward toward the cleft. Molecules of (±)-**10a** were shown to interact with each other according to the packing plot shown in Figure 3a. Thus, molecules of (±)-**10a** are linked together in a 1D polymeric H-bonded chain with amino-thiocarbamate groups forming pairs of $R^2_2(8)$, centrosymmetric N–H···S H-bond interactions to neighboring molecules (Table S1).[26,27]

Scheme 3. Preparation of Thiocarbamates (±)-10a–e and (+)-10b

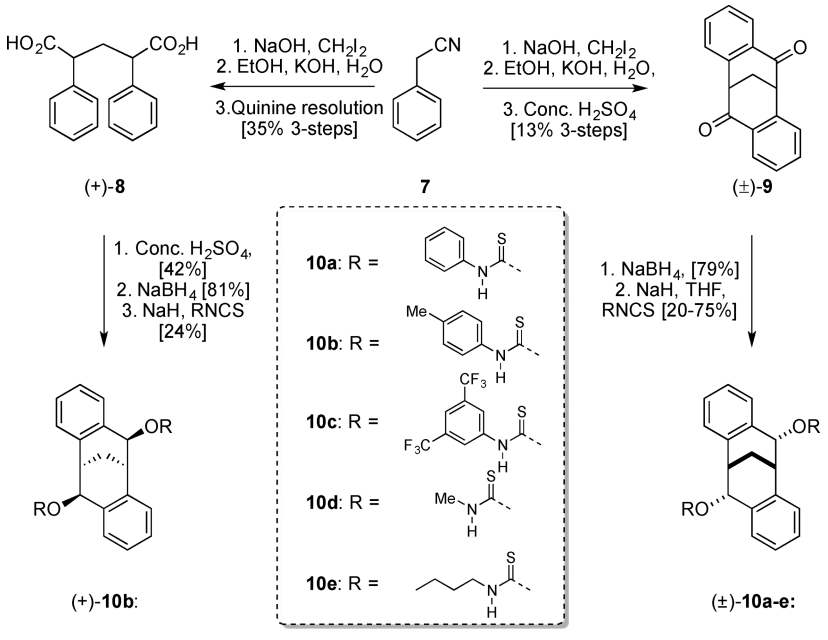

DOI: 10.1021/acs.cgd.6b00388
Cryst. Growth Des. XXXX, XXX, XXX–XXX

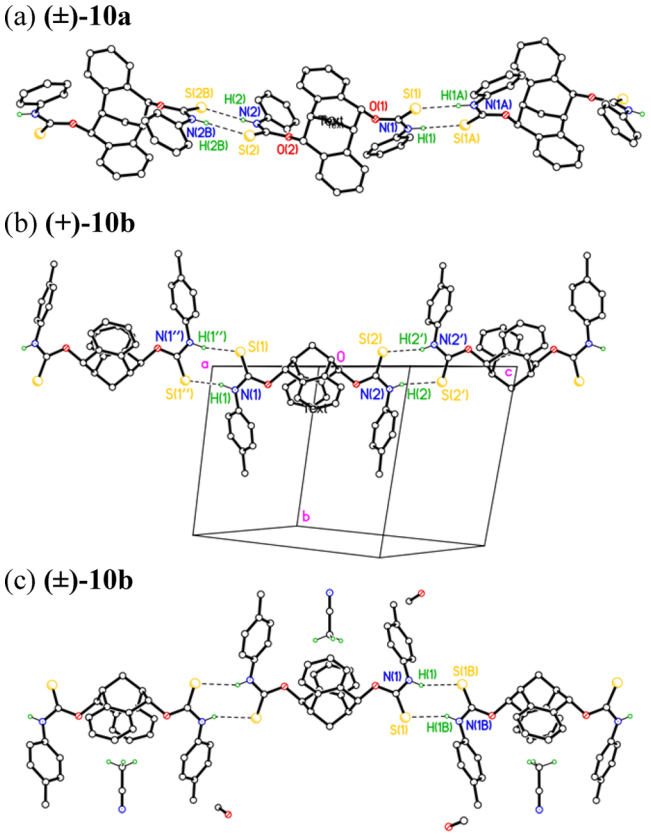

Figure 3. X-ray analysis and the H-bonded chain of (±)-**10a**, (+)-**10b**, and (±)-**10b**, respectively.

The X-ray crystal structure[28] of the (+)-enantiomer of the *p*-tolyl-amino-thiocarbamate cleft, (+)-**10b**, shows that the substituted amino-thiocarbamate groups are also directed into the cavity of the cleft bicycle with the thiocarbamate sulfur and N−H groups pointing outward away from the center of the cavity (Figures S2,3). Molecules of (+)-**10b** were bound to each other by a very similar H-bonding network as displayed in the crystal structure of (±)-**10a**. Thus, molecules are linked together via pairs of $R^2_2(8)$, centrosymmetric N−H···S H-bonds forming chains of molecules (Figure 3b, Table S2). Essentially the molecular structure of (±)-**10b** is exactly the same as that of the (+)-enantiomer with complexing *p*-tolyl-amino-thiocarbamate groups pointing into the cavity of the cleft bicycle and both the N−H and sulfur groups of the appending amino-thiocarbamate groups pointing away from the interior of the cavity.[28] Like in (+)-**10b**, this arrangement of functional groups allowed molecules to form chains linked by pairs of $R^2_2(8)$, centrosymmetric N−H···S H-bonds (Figure 3c, Table S3).

However, unlike the crystal structure of (+)-**10b**, which was found to contain crystallographically independent molecules with no solvent of crystallization, the crystal structure of the racemic compound (±)-**10b** contained solvate molecules of methanol which lie disordered over a twofold axis *exo*- to the cleft molecules. In addition, an acetonitrile solvate molecule bound via a pair of C−H···π interactions resides in the cleft cavity (Figures 3c and 4b). Interestingly, because the cleft cavity is occupied with solvent molecules bound to the cleft by moderate C−H···π interactions, neighboring H-bonded chains made up of molecules of (±)-**10b** are unable to interact as they did in (+)-**10b** where the terminal *p*-tolyl group from one chain penetrates into the cavity of the molecule in the next chain forming an "above/below"-type packing pattern (type **M2**, Figure 4a). Instead, chains of H-bonded molecules arrange into groups of six molecules which interact to form rings with the internal clefts filled with acetonitrile solvate molecules (Figure 4b).

In the crystal structure of (±)-**10c**, the fluorine atoms which make up the CF_3 groups were modeled as split over two sets of positions with one of the $C_6H_3CF_3$ groups (Figures S4,5) showing the potential to be more disordered than the others.[29] Like the other *N*-aryl functionalized amino-thiocarbamate clefts the $Ph(CF_3)_2$ substituted amino-thiocarbamate groups in (±)-**10c** are directed into the cleft cavity with the thiocarbamate sulfur and N−H groups directed away from the interior of the cleft. It would appear from X-ray packing plots that the bulky pendant fluorinated aromatic groups block the cleft cavity, preventing any interactions between the π-systems of neighboring cleft molecules. As a result, the only significant noncovalent interactions observed are H-bonds in (±)-**10c** between the thiocarbamate N−H groups and the sulfur atom of a neighboring molecule resulting in a two-dimentional H-bonded sheet via one $R^2_2(8)$ centrosymmetric motif and several chain linkages (Figure 5).

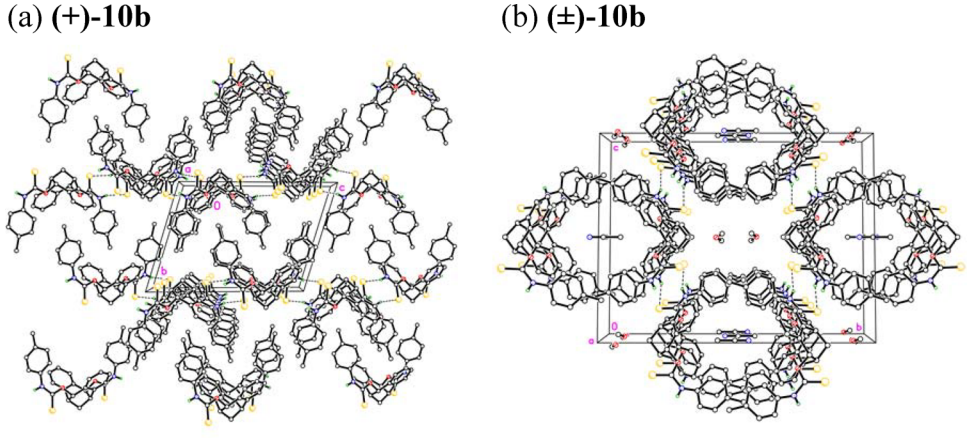

Figure 4. Comparison of the packing pattern of enantiopure and racemic **10b**; (a) (+)-**10b** showing **M2**-type packing; (b) (±)-**10b** showing **M5**-type packing.

DOI: 10.1021/acs.cgd.6b00388
Cryst. Growth Des. XXXX, XXX, XXX−XXX

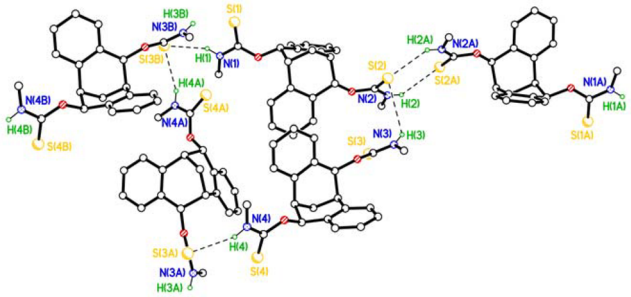

Figure 5. X-ray H-bonding analysis of (±)-**10c**. The 3,5-ditrifluoromethylphenyl groups have been omitted for clarity.

The length of the H-bonds between the sulfur and N−H groups[34] are very similar to those observed in (+)-**10b** and (±)-**10b**; however, the overall packing pattern displayed in this structure is considerably more complex due to the fluoroaryl groups.

As in the *p*-tolyl, phenyl, and fluoroaryl substituted amino-thiocarbamate groups the appending methyl-thiocarbamate groups of (±)-**10d**[28] are directed into the cavity of the cleft (Figure S6). However, unlike the *N*-aryl substituted thiocarbamate clefts mentioned previously, the thiocarbamate N−H groups in (±)-**10d** are shown to be directed into the cavity of the cleft; presumably the less bulky methyl groups facilitate this orientation. This removes the ability of the thiocarbamate N−H groups to form centrosymmetric H-bonds with neighboring clefts, as demonstrated by the clefts (+)-**10b** and (±)-**10b** (Figures 3 and 4), which appears to influence the way in which molecules of (±)-**10d** interact with each other. The packing pattern displayed by (±)-**10d** showed that molecules are linked via N−H···S H-bonds into chains/ladders, and thus the apex of one molecule is accommodated in the cleft of the next to form columns of apex-to-base stacked molecules, like a stack of party hats (type **M1**) (Table S5). The two hydrogens in the CH_2 at the bridgehead of the cleft at C(9); C(30) and C(51) (Figure 6a) make up pairs of C−H···π interactions with the cleft of the molecule "above" (Table S6). In addition to this molecular stacking pattern, this cleft presents a highly unusual cooperative packing system, where each group of three molecules is H-bonded to the next group of three molecules but with a 180° rotation between one group and the next (Figure S7).

Weakly diffracting crystals of (±)-**10e** (Figure S8) were obtained and analyzed using synchrotron radiation.[28] There were difficulties in uniquely identifying the space group, which are described in the Experimental Section. Despite these problems the identification of the compound and the nature of the stacking was clearly established (Figure 6b). The stacking adopted is the same **M1** motif adopted by the methyl analog (±)-**10d**.

From the X-ray data it is clear that the size of the R group on the thiocarbamate effects the orientation and packing of the cleft. In the case of the R being alkyl (methyl or ^{n}butyl), both thiocarbamates take on the *cisoid* conformation (Scheme 4, **6a**) and this promotes *synthon 4* giving (±)-**11d** and (±)-**11e**, respectively. This is further reinforced by weak, nonbonding interactions forming columns of two or more components with the apex of one molecule suitably aligned in the cleft of a second, and can be defined as **M1** type packing.

However, when R is an aryl group the preferred conformation of the thiocarbamate is *transoid* (**6c**) which promotes *synthon* **5** giving ribbons of clefts within the crystal

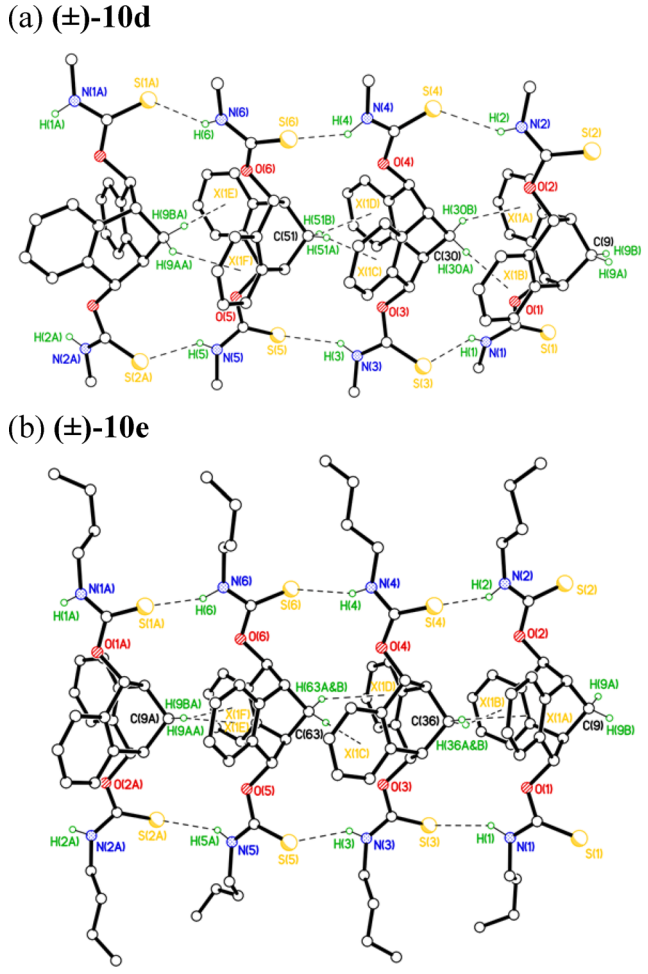

Figure 6. X-ray analysis of (±)-**10d** and (±)-**10e**, respectively, illustrating the H-bonded ladder network.

structures (±)-**11a,b** and (+)-**11b**. The packing of these ribbons in the enantiopure clefts (+)-**11b** is then controlled by the insertion of an aryl group of one cleft into the cleft of another via endoface to endoface interactions, and can be defined as **M2** type packing. In contrast, in the racemic series (±)-**11a,b** the packing of these ribbons gives rise to a new motif **M5**, which promotes the formation of rings with the internal clefts filled with acetonitrile solvate molecules. Clearly this latter network provides the opportunity to form other host:guest complexes using these channels. Finally, the 3,5-CF_3Ph thiocarbamate (±)-**10c**, which contains bulky pendant fluorinated aromatic groups that block the cleft cavity, presumably forms networks using the *cisoid* (**6a**), *transoid* (**6c**), or mixtures of both forms (**6b**), giving a disordered H-bonded network.

CONCLUSIONS

Through using a combination of a novel chiral cleft molecule and thiocarbamates we have demonstrated that we can control the crystal packing by simple variation of the size of the substituent on the thiocarbamate. This has been achieved due to the tendency of the C_2-symmetric cleft to form molecule associations within the solid state described as **M1**−**M4**, and thiocarbamates to form synthons via their *cisoid* and *transoid* conformers. Smaller substituents lead to H-bonding in the thiocarbamate in its *cisoid* form, and this is further strengthened

DOI: 10.1021/acs.cgd.6b00388
Cryst. Growth Des. XXXX, XXX, XXX−XXX

Scheme 4. Role of the Thiocarbamate in Determining Crystal Structure and the H-Bonded Network

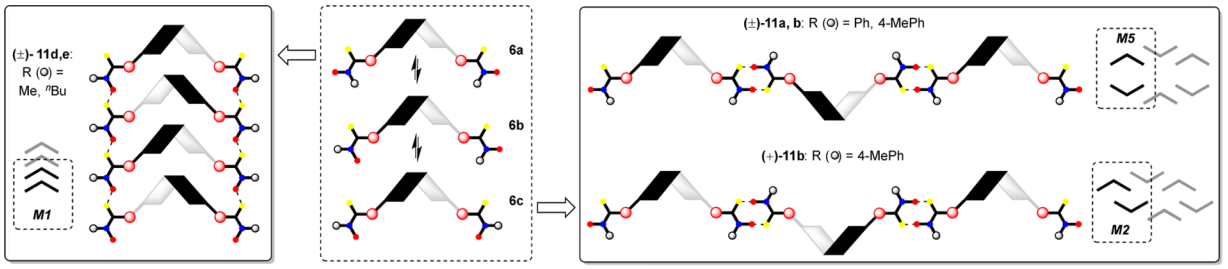

by type **M1** interactions. Larger substituents such as phenyl and tolyl lead to H-bonding ribbon type networks via the *transoid* form of the thiocarbamate. However, we have demonstrated that the packing of these ribbons differs significantly between the racemic and enantiopure clefts, with the racemic series giving rise to channels within the crystal structure, via a new type of interaction **M5**. Moreover, the crystal structure of **(±)-10b** provided evidence of the ability of these novel amino-thiocarbamate clefts to bind guest molecules with complementary size and binding features. Interestingly, binding within the cleft cavity was facilitated by C−H···π H-bond interactions originating from the core carbocyclic cleft framework, and supported by H-bonds involving the thiocarbamate groups. Given that cleft **1** is C_2-symmetric, this simple but effective control of crystallization within the solid state has significant potential to be expanded upon using other hydrogen bond synthons.

EXPERIMENTAL SECTION

General Procedure for the Preparation of Amino-Thiocarbamate Clefts. Sodium hydride (60% mineral oil, 4.0 mmol) was washed with hexane (3 × 10 mL) and dried under vacuum, THF (10 mL) was added and the suspension was cooled to 0 °C. Racemic **(±)-1** or **(+)-1** (1.0 mmol) was dissolved in THF (5 mL) and added to the sodium hydride suspension via a cannula under nitrogen and the reaction was stirred at 0 °C for 25 min. After this time a solution of substituted isothiocyanate (3.0 mmol) in THF (5 mL) was added dropwise to the reaction mixture. The solution was allowed to warm to room temperature and then stirred for a further 18 h; reactions were monitored by TLC. After this time the reaction was quenched by the careful addition of water (20 mL) and extracted with dichloromethane (3 × 25 mL). The combined organic layers were washed with brine (25 mL), dried over $MgSO_4$, filtered, and concentrated to dryness in vacuo. The crude compound was purified by silica column chromatography.

*(±)-2,8-Dibenzobicyclo [b,f] [3.3.1]nona-**5a,6a**-dien-6,12-phenylaminothiocarbamate (±)-**10a**.* (0.2 g, 57%), fine white solid; Mp 111.6−114.7 °C; ^{1}H NMR (400 MHz, $CDCl_3$): δ 7.74−7.00 (m, 20 H), 3.91−3.88 (m, 2H), 2.60−2.58 (m, 2H); ^{13}C NMR (100 MHz, $CDCl_3$): δ 188.41, 136.86, 136.65, 134.61, 133.96, 130.67, 130.48, 129.04, 127.66, 127.47, 126.77, 125.26, 121.42, 83.74, 72.59, 39.22, 35.62, 29.08; IR CH_2Cl_2 max/cm^{-1}: 3943, 3584, 3361 (N−H), 3054, 2986 (aromatics), 2305, 1526, 1265, 1160, 1034, 743, 705; HRMS *m/z* found 545.1327 $C_{31}H_{26}O_2N_2S_2$ (M^+ Na) expected 545.1328 (M^+ Na); Elemental Analysis found C 71.06; H 4.98; N 5.41% $C_{31}H_{26}N_2O_2S_2$ requires C 71.24; H 5.01; N 5.36%.

*(±)-2,8-Dibenzobicyclo [b,f] [3.3.1]nona-**5a,6a**-dien-6,12-p-tolylaminothiocarbamate (±)-**10b**.* (0.4 g, 70%) fine white solid; Mp 209.9−211.2 °C; ^{1}H NMR (400 MHz, $CDCl_3$): δ 7.58 (d, *J* = 8.4 Hz, 2H), 7.29−7.15 (m, 7H), 7.09 (d, *J* = 7.2 Hz, 2H), 7.04−6.84 (m, 7H), 3.89 (m, 2H), 2.58 (m, 2H), 2.41 (s, 3H), 2.28 (s, 3H); ^{13}C NMR (100 MHz, $CDCl_3$): δ 188.30, 136.32, 135.36, 134.92, 134.83, 133.85, 131.05, 129.72, 129.54, 127.39, 127.11, 126.55, 123.59, 121.47, 83.37, 79.45, 46.00, 35.36, 20.93; IR CH_2Cl_2 max/cm^{-1}: 3944 (s, N−H), 3689 (s, N−H), 2986 (aromatics), 2305, 1520, 1265, 739, 704; HRMS *m/z* found 573.1639 $C_{33}H_{30}O_2N_2S_2$ (M^+ Na) expected 573.1641 (M^+ Na); Elemental analysis found C 71.55; H 5.46; N 5.13%; $C_{33}H_{30}N_2O_2S_2$ requires C 71.97; H 5.49; N 5.09%.

*(+)-2,8-Dibenzobicyclo [b,f] [3.3.1]nona-**5a,6a**-dien-6,12-p-tolylaminothiocarbamate (+)-**10b**.* (0.26 g, 24%), fine white solid; Mp 116.2−124.7 °C; $[\alpha]_D^{21}$ + 174.3 (*c* 1.0, $CHCl_3$); ^{1}H NMR (400 MHz, $CDCl_3$): δ 7.47 (d, *J* = 7.6 Hz, 2H), 7.17−7.08 (m, 7H), 6.95 (d, *J* = 5.2 Hz, 2H), 6.89−6.75 (m, 7H), 3.79 (m, 2H), 2.46 (m, 2H), 2.30 (s, 3H), 2.14 (s, 3H); ^{13}C NMR (100 MHz, $CDCl_3$): δ 188.21, 136.36, 134.84, 134.30, 131.08, 129.61, 129.54, 127.14, 126.56, 123.63, 121.52, 83.34, 79.44, 35.42, 28.82, 20.99; IR CH_2Cl_2 max/cm^{-1}: 3944, 3054 (N−H), 2986 (aromatics), 2305, 1522, 1265, 1171, 1034, 739, 704; HRMS *m/z* found 573.1642 $C_{33}H_{30}O_2N_2S_2$ (M^+ Na) expected 573.1641 (M^+ Na); Elemental analysis found C 71.79; H 5.57; N 5.16%; $C_{33}H_{30}N_2O_2S_2$ requires C 71.97; H 5.49; N 5.09%.

*(±)-2,8-Dibenzobicyclo [b,f] [3.3.1]nona-**5a,6a**-dien-6,12-bis-3,5-bis(trifluoromethyl)phenylaminothiocarbamate (±)-**10c**.* (0.70 g, 44%), off-white solid; Mp 120.1−127.4 °C; ^{1}H NMR (400 MHz, $CDCl_3$): δ 8.00−6.20 (m, 14H), 3.85 (s, 2H), 1.44 (s, 2H; ^{13}C NMR (100 MHz, $CDCl_3$): δ 194.42, 140.05, 134.52, 128.85, 138.83, 128.79, 128.30, 48.82, 32.33; IR CH_2Cl_2 max/cm^{-1}: 3204, 3055 (N−H), 2987 (aromatics), 2306, 1551, 1139, 1265, 1031, 738, 703; HRMS *m/z* found 817.0777 $C_{35}H_{22}O_2N_2S_2F_{12}$ (M^+ Na) expected 817.0823 (M^+ Na); Elemental analysis found C 52.34; H 2.77; N 3.72% $C_{35}H_{22}F_{12}N_2O_2S_2$ requires C 52.90; H 2.79; N 3.53%.

*(±)-2,8-Dibenzobicyclo [b,f] [3.3.1]nona-**5a,6a**-dien-6,12-methylaminothiocarbamate (±)-**10d**.* (0.60 g, 75%), colorless solid; Mp 212.1−218.2 °C; ^{1}H NMR (400 MHz, $CDCl_3$): δ 7.12−7.04 (m, 8H), 6.79 (dd, *J* = 6.8 Hz, 1H), 6.35 (dd, *J* = 6.0 Hz, 1H), 3.74 (m, 1H), 3.66 (m, 1H), 3.13 (t, *J* = 5.2 Hz, 6H) 2.64 (d, *J* = 5.2 Hz, 1H), 2.53 (d, *J* = 5.2 Hz, 1H), 1.97 (m, 2H); ^{13}C NMR (100 MHz, $CDCl_3$): δ 194.1 90.09, 135.52, 135.43, 135.26, 134.88, 130.98, 127.36, 127.31, 127.20, 126.99, 126.81, 126.77, 126.71; IR CH_2Cl_2 max/cm^{-1}: 3399 (N−H), 3052 (aromatics), 1528, 1265, 1068, 737, 703; HRMS *m/z* found 421.1013 $C_{21}H_{22}O_2N_2S_2$ (M^+ Na) expected 421.1015 (M^+ Na); Elemental analysis found C 63.07; H 5.58; N 6.99% $C_{21}H_{22}N_2O_2S_2$ requires C 63.29; H 5.56; N 7.03%.

DOI: 10.1021/acs.cgd.6b00388
Cryst. Growth Des. XXXX, XXX, XXX−XXX

*(±)-2,8-Dibenzobicyclo [b,f] [3.3.1]nona-**5a,6a**-dien-butylaminothiocarbamate (±)-**10e**.* (0.19 g, 20%), colorless solid; Mp 213.3−214.4 °C; ^{1}H NMR (400 MHz, $CDCl_3$): δ 7.46−6.70 (m, 12H), 5.01 (m, 2H), 3.74 (s, 1H), 3.31 (s, 1H), 2.49−2.36 (m, 2H), 2.25 (S, 3H); ^{13}C NMR (100 MHz, $CDCl_3$): δ 188.51, 130.59, 129.56, 127.63, 127.44, 126.73, 121.50, 83.63, 72.60, 39.22, 35.61, 29.09, 21.31; IR CH_2Cl_2 max/cm^{-1}: 3257 (N−H), 2957, 2931 (aromatics), 1519, 1179, 1038, 752; HRMS *m/z* found 505.1954 $C_{27}H_{34}O_2N_2S_2$ (M^+ Na) expected 505.1954 (M^+ Na); Elemental analysis found C 66.96; H 7.02; N 5.73% $C_{25}H_{23}NO_2S$ requires C 67.18; H 7.10; N 5.80%.

X-ray Crystallography. Diffraction data for **(±)-10a·CHCl$_3$** and **(±)-10b·MeOH·CH$_3$CN**, and were collected on a Bruker APEX 2 CCD diffractometer equipped with graphite-monochromated Mo Kα X-radiation. Diffraction data for **(+)-10b**, **(±)-10c·0.25C$_5$H$_{12}$**, and **(±)-10d** and were collected on a Bruker APEX 2 CCD diffractometer equipped with a silicon 111 monochromator using narrow frame ω-scans on Station 11.3.1 at the ALS using synchrotron radiation.[30] Data for **(±)-10e** were also collected at the ALS but with a Bruker D8 diffractometer with a CMOS detector using shutterless ω-scans. Data were corrected for absorption and Lp effects.[30] Structures were solved by direct methods or charge flipping algorithms[31,32] and refined by full-matrix least-squares on F^2.[33] Further details are given in Table 7 in the SI. In **(±)-10a·CHCl$_3$** the $CHCl_3$ molecule was modeled as disordered over two sets of positions with major component 63.6(6)%. In **(±)-10b·MeOH·CH$_3$CN** the MeOH molecule is disordered over a twofold axis and the O*H* position could not be reliably determined, so it was not refined. In **(±)-10c·0.25C$_5$H$_{12}$** there are two cleft molecules in the asymmetric unit, both exhibiting disorder. CF_3 groups at C(26), C(34), C(35), C(69), and C(70) were all modeled as twofold disordered, as were the ring atoms C(54) > C(57) and the CF_3 group at C(60). The badly disordered partial pentane of crystallization was modeled as a diffuse area of electron density by the Platon Squeeze procedure.[34] The structure of **(±)-10e** is presented as provisional due to the severe crystallographic problems encountered associated with space group ambiguity. Data sets were collected both in the home laboratory and at the ALS synchrotron. In both cases the same unit cell parameters were obtained. Crystal data for **(±)-10e**: $C_{27}H_{34}N_2O_2S2$, M = 482.68, monoclinic, *Pc* (or $P2_1/c$), a = 12.2150(11), b = 26.553(2), c = 24.029(2)Å, β = 99.357(5)°, V = 7690.0(11) Å^3, Z = 12, μ = 0.234 mm^{-1}, 77 800 reflections measured, 25961 unique, R_{int} = 0.0749, $R_1[F^2 > 2\sigma(F^2)]$ = 0.2110. Similarity restraints were applied to the geometry of all molecules and global restraints were required for anisotropic displacement parameters. Six molecules in the asymmetric unit in two groups of three for space group *Pc*, which gave the best result (one group of three in space group $P2_1/c$). N−H···S H-bonds in the range 3.28(2)−3.541(13) Å and C−H···π distances in the range 2.41−2.75 Å.

■ ASSOCIATED CONTENT

Supporting Information

The Supporting Information is available free of charge on the ACS Publications website at DOI: 10.1021/acs.cgd.6b00388.

Experimental procedures for the synthesis of **(+)-9**, **(−)-9**, **(±)-9**, as well as the HPLC traces of **(+)-9**, **(−)-9**, and **(±)-9**. Spectroscopic data for all reported compounds. Table S1 contains the crystallographic data for **(±)-10a**, **(+)-10b**, **(±)-10b**, **(±)-10c**, and **(±)-10d**. Tables S2−S7 contain selected H-bonded geometries for **(±)-10a**, **(+)-10b**, **(±)-10b**, **(±)-10c**, and **(±)-10d**, respectively. Figures S1−S6 contains ORTEP plots of **(±)-10a**, **(+)-10b**, **(±)-10b**, **(±)-10c**, and **(±)-10d** (two molecules), respectively. Figure S7 depicts the H-bonding network of **(±)-10c**, and Figure S8 the H-bonding network of **(±)-10e**. (PDF)

Accession Codes

CCDC 1441482−1441486 contains the supplementary crystallographic data for this paper. These data can be obtained free of charge via www.ccdc.cam.ac.uk/data_request/cif, or by emailing data_request@ccdc.cam.ac.uk, or by contacting The Cambridge Crystallographic Data Centre, 12, Union Road, Cambridge CB2 1EZ, UK; fax: +44 1223 336033.

■ AUTHOR INFORMATION

Corresponding Authors

*E-mail: M.R.J.Elsegood@lboro.ac.uk. Tel. +44 (0) 1509 22 8751.

*E-mail: M.C.Kimber@lboro.ac.uk. Tel. +44 (0) 1509 22 2570.

Notes

The authors declare no competing financial interest.

■ ACKNOWLEDGMENTS

We gratefully acknowledge financial support from Loughborough University (studentship for NHS). We also thank Dr. Mark Edgar (Loughborough) for assistance with NMR assignments. The Advanced Light Source is supported by the Director, Office of Science, Office of Basic Energy Sciences, of the U.S. Department of Energy under Contract No. DE-AC02-05CH11231.

■ REFERENCES

(1) Stetter, H.; Reischl, A. *Chem. Ber.* **1960**, *93*, 791.

(2) Tatemitsu, H.; Ogura, F.; Nakagawa, Y.; Nakagawa, M.; Naemura, K.; Nakazaki, M. *Bull. Chem. Soc. Jpn.* **1975**, *48*, 2473.

(3) For a review, see: Turner, J. J.; Harding, M. M. *Supramol. Chem.* **2005**, *17*, 369.

(4) Friberg, A.; Olsson, C.; Ek, F.; Berg, U.; Frejd, T. *Tetrahedron: Asymmetry* **2007**, *18*, 885.

(5) Field, J. D.; Turner, P.; Harding, M. M.; Hatzikominos, T.; Kim, L. *New J. Chem.* **2002**, *26*, 720.

(6) Anderberg, P. I.; Turner, J. J.; Evans, K. J.; Hutchins, L. M.; Harding, M. M. *J. Chem. Soc., Dalton Trans.* **2004**, 1708.

(7) Lee, C. K. Y.; Groneman, J. L.; Turner, P.; Rendina, L. M.; Harding, M. M. *Tetrahedron* **2006**, *62*, 4870.

(8) Naemura, K.; Fukunaga, R. *Chem. Lett.* **1985**, 1651.

(9) Naemura, K.; Fukunaga, R.; Yamanaka, M. *J. Chem. Soc., Chem. Commun.* **1985**, 1560.

(10) Naemura, K.; Fukunaga, R.; Komatsu, M.; Yamanaka, M.; Chikamatsu, H. *Bull. Chem. Soc. Jpn.* **1989**, *62*, 83.

(11) Thunberg, L.; Allenmark, S.; Friberg, A.; Ek, F.; Frejd, T. *Chirality* **2004**, *16*, 614.

(12) Try, A. C.; Painter, L.; Harding, M. M. *Tetrahedron Lett.* **1998**, *39*, 9809.

(13) Kimber, M. C.; Try, A. C.; Painter, L.; Harding, M. M.; Turner, P. *J. Org. Chem.* **2000**, *65*, 3042.

(14) Jilka, P.; Millington, C.; Elsegood, M. R. J.; Frese, J. W. A.; Teat, S.; Kimber, M. C. *Tetrahedron* **2010**, *66*, 9327.

(15) Elsegood, M. R. J.; Kimber, M. C. *Tetrahedron Lett.* **2015**, *56*, 346.

(16) For recent reviews in the area of crystal engineering see Mukherjee, A. *Cryst. Growth Des.* **2015**, *15*, 3076.

(17) Desiraju, G. R. *J. Am. Chem. Soc.* **2013**, *135*, 9952.

DOI: 10.1021/acs.cgd.6b00388
Cryst. Growth Des. XXXX, XXX, XXX−XXX

(18) Christer, B.; Aakeröy, C. B.; Champness, N. R.; Janiak, C. *CrystEngComm* **2010**, *12*, 22.
(19) Mann, S. *Nature* **1993**, *365*, 499.
(20) Hosseini, M. W. *CrystEngComm* **2004**, *6*, 318.
(21) Hosseini, M. W.; De Cian, A. *Chem. Commun.* **1998**, 727.
(22) Hossieni, M. W. *Acc. Chem. Res.* **2005**, *38*, 313.
(23) Tröger, J. *J. Prakt. Chem.* **1887**, *36*, 225.
(24) Rúnarsson, Ö. V.; Artacho, J.; Wärnmark, K. *Eur. J. Org. Chem.* **2012**, *2012*, 7015.
(25) Cross, J. T.; Rossi, N. A.; Serafin, M.; Wheeler, K. A. *CrystEngComm* **2014**, *16*, 7251.
(26) Etter, M. C. *Acc. Chem. Res.* **1990**, *23*, 120.
(27) Bernstein, J.; Davis, R. E.; Shimoni, L.; Chang, N.-L. *Angew. Chem., Int. Ed. Engl.* **1995**, *34*, 1555.
(28) Due to small crystal dimensions this data set was collected using synchrotron radiation at the ALS.
(29) Modeled with atoms C(54) > C(57), C(60) and F(13) > F(15).
(30) APEX 2 and SAINT (2012) software for CCD diffractometers; Bruker AXS Inc., Madison, USA.
(31) Sheldrick, G. M. *Acta Crystallogr., Sect. A: Found. Crystallogr.* **2008**, *A64*, 112.
(32) Sheldrick, G. M. *Acta Crystallogr., Sect. A: Found. Adv.* **2015**, *A71*, 3.
(33) Sheldrick, G. M. *Acta Crystallogr.* **2015**, *C71*, 3.
(34) Spek, A. L. *Acta Crystallogr., Sect. C: Cryst. Struct. Commun.* **1990**, *A46*, 1357.

DOI: 10.1021/acs.cgd.6b00388
Cryst. Growth Des. XXXX, XXX, XXX−XXX